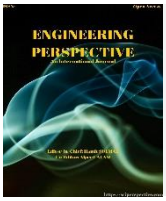

e-ISSN:2757-9077

ENGINEERING PERSPECTIVE

https://sciperspective.com/ Research Paper

Working Fluid Selection and Performance Analysis for the Afyon Geothermal Energy Plant

Ömer Faruk Güler[1*]

[1] *Mechanical Engineering Department, Faculty of Technology, Afyon Kocatepe University, Afyonkarahisar, 03200, Türkiye*

ABSTRACT

Renewable energy production has been steadily increasing in recent years. Generating energy from renewable sources and making them operational for use is essential. Alongside production, efficiently utilizing these resources is equally important. For efficient use, exploring various alternatives and conducting optimization processes are crucial. Organic Rankine Cycles (ORCs) allow energy production from low-enthalpy temperature sources. By using working fluids with low boiling points, it is possible to create a Rankine cycle at low temperatures. Each system operates under unique regional and environmental conditions, so careful selection of working fluids is necessary. Factors such as heat source temperature and pressure, ambient pressure and temperature, location, and purpose of use cause different fluids to exhibit varying behaviors. In this study, the effects of different working fluids were examined for the Afyon geothermal power plant. The active plant utilizes geothermal water at 110°C and a flow rate of 150 kg/s. The plant's capacity is approximately 2.7 MW. R-134a, a widely used working fluid, serves as the intermediary fluid. Additionally, fluids such as isopentane, n-pentane, isobutane, R-12, and R-32 were tested. Thermodynamic and thermoeconomic analyses of the system were conducted using these fluids. With R-134a, 2.75 MW of power was generated at a unit energy cost of $0.025/kWh. Among the alternative fluids, isobutane produced 2.95 MW of power with a unit energy cost of $0.016/kWh. The energy efficiencies of the system for R-134a and isobutane were 10.9% and 11.6%, respectively. Similarly, the exergy efficiencies for these fluids were 31.1% and 33.1%, respectively. Although better results can be achieved with certain alternative fluids, the data are insufficient to directly replace the current working fluid in the system. Performing a separate optimization study with these promising fluids will be a critical step in determining the final working fluid.

Keywords: Geothermal Energy; ORC; Thermo-Economic Analysis; Working Fluid Selection

History
Received: 04.05.2024
Accepted: 26.11.2024

Author Contacts
**Corresponding Author*
e-mail addresses : ofguler@aku.edu.tr,

How to cite this paper: Güler, Ö.F. (2025). Working Fluid Selection and Performance Analysis for the Afyon Geothermal Energy Plant. Engineering Perspective, 5 (1), 1-8. http://dx.doi.org/10.29228/eng.pers.80205

1. Introduction

Energy efficiency and renewable energy applications have made significant progress. These advancements, particularly in the efficient use of renewable resources for maximum utilization. Also, they are continuing to grow. One of these is the Organic Rankine Cycle (ORC). ORC enables the use of low-enthalpy energy sources. These sources may include waste heat from a heat-utilizing facility or heat derived from a renewable source such as solar or geothermal energy. Historically, high-enthalpy geothermal resources were the first to be utilized in Rankine Cycles [1]. Later, the idea of harnessing low-enthalpy sources led to the use of alternative working fluids instead of water vapor in Rankine cycles. These fluids, with lower boiling point temperatures, have rapidly increased the exploitation of low-temperature renewable resources. Organic fluids are used as the working medium in such systems. Various fluid types exist, each with diverse thermophysical properties. Choosing the most suitable working fluid for each system is important, and the literature includes various studies on this topic.

Optimizing waste heat recovery is an important research area for making renewable energy resources more productive. The working fluids used in ORC systems significantly influence system efficiency, environmental impact, and economic performance. Comparing different working fluids is thus a vital step toward improving ORC energy plant performance. Many studies emphasize using low-global warming potential (GWP) working fluids to reduce environmental impacts. Wang et al. [2] compared the thermodynamic performance of various low-GWP fluids used in ORC systems and highlighted the advantages of these fluids in recovering low-temperature waste

heat. They noted that fluids such as R245fa and isopentane are more environmentally friendly options [3]. Additionally, the use of fluid mixtures has been shown to provide more efficiency compared to pure fluids. These mixtures enable higher energy production and greater exergy efficiency in ORC systems while improving electricity generation costs.

Some of the other researches focus on Multi-objective optimization of the energy plant. Multi-objective optimization processes are employed to make ORC systems more economically and environmentally efficient. These optimizations are try to enhance both thermodynamic efficiency and economic performance. For instance, Li et al.[4] investigated the integration of LNG cold energy and geothermal energy to enhance ORC system performance, achieving a 43.3% efficiency improvement through multi-objective optimization. Such optimization processes improve the design and operational parameters of systems.

Another important application is the integration of ORC systems into reversible heat pump systems. These systems, often utilizing multiple energy sources, both hot and cold, offer multipurpose applications to improve heat recovery efficiency. For example, Daniarta et. al. [5] offer an ORC system integrated with a reversible heat pump that demonstrated significant efficiency improvements, depending on system design and working fluid selection. These kinds of systems are particularly effective in reducing energy production costs by utilizing waste heat recovery and low-temperature sources, as for example achieving energy savings of up to 50%, according to this study.

In optimizing ORC system performance, choosing working fluid plays an important role. Xia et al. [6] used multi-objective optimization approaches to analyze the performance of ORC-VCR (Organic Rankine Cycle-Vapor Compression Refrigeration) systems. They tried to demonstrate the significant impact of fluid mixtures on system efficiency. These studies also identified the necessary parameters for enhancing ORC systems' efficiency under different temperature and pressure conditions. Furthermore, economic performance analyses of ORC systems with various fluids are a major research area. Feng et al. [7] examined ORC systems in an economical way. They explained how fluid selection affects electricity generation and cost. They showed that fluid mixtures offer more cost-effective solutions than pure fluids, reducing energy generation costs. Similarly, Liang et al. [8] optimized ORC cycles in thermal integrated pumped thermal energy storage (TIPTES) systems using different working fluids, ultimately selecting the most suitable fluid for their system. They used R-245fa, Isobutane, Isopentane, MM and R1336mzz(Z)— as a working fluid. Similarly, in their study, Rachmat and colleagues [9] aimed to propose a new configuration for Unit 2 of the Wayang Windu geothermal power plant by integrating a double-flash separator with an ORC system. The analysis, conducted using R245fa as the working fluid, was evaluated both thermodynamically and economically and compared with the existing system. As a result of the optimization, the exergy efficiency was found to be 54.40%, the specific cost $1.86/GJ, and the payback period 0.32 years. This configuration offers some improvements over the existing system in both thermodynamic and economic terms. Also, another research topic is the optimization of hybrid systems. The hybrid systems integrate different energy sources or different power cycles. Li et al. [4] demonstrated the effectiveness of multi-objective optimizations in such hybrid systems by investigating ORC and LNG cold energy integration. These hybrid systems enhance the efficiency of the system, thus providing environmental and economic benefits.

Optimizing an ORC can help reduce the environmental side effects of energy plants. Hou et al. [10] optimized ORC technology for low-temperature waste heat recovery in ammonia synthesis plants, reducing cyclical water consumption and improving exergy performance. With optimal conditions, exergy efficiency increased by 35.53%, electricity production costs decreased by $0.043, and annual CO_2 emissions were reduced by 3,736.30 tons.

As a result, the importance of optimization studies cannot be ignored, as they have the potential to enhance the efficiency of ORC systems through improved system design and parameter adjustments. Exergoeconomic analyses are also valuable for optimizing both energy efficiency and economic performance. Numerous studies predict that the methods employed to improve the economic and environmental performance of ORC systems will increase their applicability in future projects [11].

Afyonkarahisar province is abundant in geothermal energy. Electricity is generated from the geothermal power plant established in the region. Lately, researchers have conducted various analyses of this power plant. Şahin performed the thermodynamic analysis of the Afyon geothermal power plant, which uses an ORC with R-134a as the working fluid [12]. Yılmaz later conducted a similar analysis of the same plant, modeling with three different working fluids: R-134a, n-Pentane, and Isobutane [13]. In another study, he used the results of his previous work and suggested that optimization could be achieved [14]. He tried to explain plant characteristics with some parametric results. However, the analysis of the fluids was not explored in detail in Yılmaz's studies. Building on these valuable contributions, the current study investigates the effects of different working fluids. Six different working fluids were tested: R-134a, Isopentane, n-Pentane, R-12, Isobutane, and R-32. The pressure and temperature values were carefully selected based on the properties of each fluid. The evaporation temperature was adjusted to be as close as possible to the maximum temperature achievable in the heat exchanger, while the condensation temperature was brought as close as possible to the cooling water temperature. This approach allows for a clearer assessment of the newly tested working fluids. The ability of these systems to adapt to a broader range of applications is crucial for achieving future energy transformation and sustainability goals.

2. Method

The thermodynamic model of the existing geothermal power plant in Afyonkarahisar province will be developed, and detailed analyses of this model will be conducted. Initially, a schematic representation of the power plant will be created, highlighting the essential components. Subsequently, calculations related to these components will be presented separately, addressing both thermodynamic and economic aspects. These are grouped under three subheadings; system description, thermodynamic analysis, thermo-economic analysis.

2.1 System description

The system consists of an ORC cycle stream, a geothermal water flow, and a cooling water flow. The ORC cycle includes a turbine, a condenser, a heat exchanger, and a pump.

Cooling water is used in the condenser, matching the current

power plant's data. The use of water ensures stable cooling at a constant temperature throughout the year, unlike air-cooled systems, which consume more energy. The region experiences significant temperature differences between summer and winter, as well as day and night. Using air for cooling creates additional challenges due to fluctuating temperatures. During the summer, when temperatures rise, the efficiency of the plant already operating at low temperatures can drop significantly with air cooling.

The system's heat input comes from a geothermal source. Although the source temperature varies slightly depending on the wells, it averages around 110°C. The water flow rate is 150 kg/s. Due to the high mineral content and low enthalpy of the water, direct usage is not feasible. Instead, a heat exchanger is used to transfer heat into the system. With the current setup, a temperature difference of 10°C (K) is achieved to transfer this heat in heat exchanger.

A pump is used to maintain system pressure, and a turbine is included for energy generation. The isentropic efficiencies of the turbine and pump are considered as 85% in calculations [15].

A schematic diagram of the system is presented in Figure 1. In the diagram, the red stream represents geothermal water, the green stream indicates the organic fluid flow, and the blue stream shows the cooling water flow. The system is modeled and analyzed as control volumes, with each control volume assigned a state number. The states are defined as follows: between the pump and condenser (1), between the pump and heat exchanger (2), between the heat exchanger and turbine (3), at the turbine outlet and condenser inlet (4), geothermal water inlet (5), geothermal water outlet from the heat exchanger (6), and cooling water inlet and outlet (7 and 8, respectively).

The analyses are divided into two main sections: thermodynamic and exergoeconomic analyses. The thermodynamic analysis includes energy and exergy assessments for each control volume. The exergoeconomic analysis builds on the thermodynamic results to perform economic evaluations.

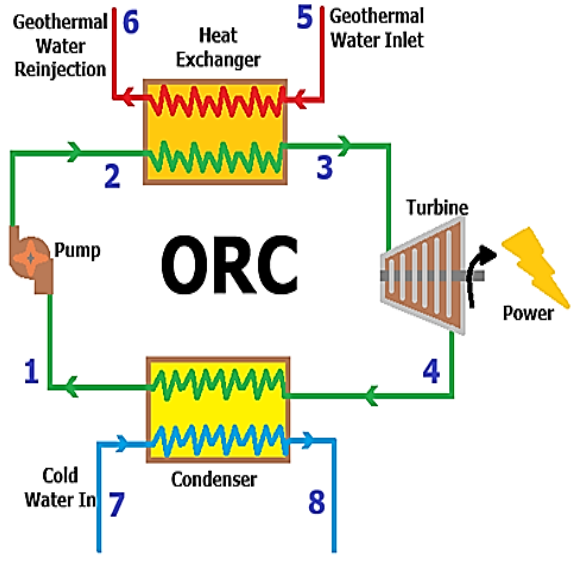

Figure 1. Schematic diagram of Afyon Geothermal Plant

2.2 Thermodynamic Analysis

In the thermodynamic analyses, energy and exergy calculations were performed for each component. EES software was used to perform these analyses. The energy equations for the equipment in the system, such as the pump, heat exchanger, turbine, and condenser, are presented sequentially according to their system state numbers.

The work required for pumping is calculated using Equation (1) [16].

$$\dot{w}_p = \frac{v_1 (P_2 - P_1)}{\eta_p} \quad (1)$$

After calculating pump work, h_2 value can be calculated be calculated by adding this work to h_1, as in Equation (2) [16].

$$h_2 = h_1 + \dot{w}_p \quad (2)$$

Enthalpy equity can be written for the heat transferred in heat exchanger like in Equation (3) [16].

$$m_{geo} (h_5 - h_6) = m_{wf} (h_3 - h_2) \quad (3)$$

Turbin work is calculated according to isentropic efficiency of the turbine (Equations (4),(5)) [16].

$$\dot{w}_T = h_3 - h_4 \quad (4)$$

$$\eta_T = \frac{\dot{w}_T}{\dot{w}_{T,iso}} = \frac{h_3 - h_4}{h_3 - h_{4,s}} \quad (5)$$

Finally, cycle waste heat is removed from the condenser. In Eqn. (6), again, the calculation is made like the heat exchanger [16].

$$m_{water} (h_8 - h_7) = m_{wf} (h_4 - h_1) \quad (6)$$

The exergy of a flow is calculated as in Equations (7) and (8) [16].

$$ex_i = (h_i - h_0) - T_0 (s_i - s_0) \quad (7)$$

$$\dot{Ex}_i = \dot{m}_i . ex_i \quad (8)$$

2.3 Thermo-economic analysis

In the economic analysis, the annual operating time is assumed to be 7,200 hours, equivalent to approximately 300 days of activity per year. The total lifespan of the facility is considered to be 10 years. An interest rate of 5% and maintenance and operating costs of 6% are assumed.

The cost recovery factor is calculated using the following Egn. (9) [17].

$$CRF = \frac{i.(i+1)^n}{(i+1)^n - 1} \quad (9)$$

The annual levelized cost of a component is found with Equation. (10) [17].

$$\dot{Z}_{CI,k} = CRF.C_{I,k} \quad (10)$$

Similarly, maintenance and repair costs are found from Equation (11) [17].

$$\dot{Z}_{OM,k} = CRF.C_{I,k}.\varphi \quad (11)$$

The total component levelized cost is found by the Equation (12) [17].

$$\dot{Z}_{Total,k} = \dot{Z}_{OM,k} + \dot{Z}_{CI,k} \quad (12)$$

The cost of a flow is obtained by multiplying the unit exergy cost of the flow by the exergy (Equation (13) [17].

$$\dot{C}_i = E\dot{x}_i.c_i \quad (13)$$

For any component, when the exergy flows entering and leaving the component, as well as the component-specific cost, are included, the economic equation takes the form of Equation (14). Its schematic can be seen in Figure 2. Here, there may be multiple inlets and outlets. For example, a heat exchanger has two inlet streams and two outlet streams. However, the method of the calculation will not change. The input costs and component costs will be written on one side, while the output costs will be written on the other side of the equation [17].

$$\dot{C}_{i,inlet} + Z_{Total,k} = \dot{C}_{i,outlet} \quad (14)$$

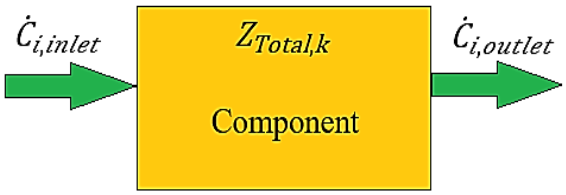

Figure 2. Economic analysis of a component

The cycle components can be adapted individually to Eguation (14). When applied to the pump, Equation (15) is obtained. Here, the $\dot{C}_1$ value used in the calculation of the c_1 value is determined based on the cost of the working fluid. Various values for different working fluids are available in the literature. However, most of these values exhibit variability. To avoid a significant manipulation on the unit cost, an average value of 6 $/GJ, which is the same for all fluids, has been adopted. This value largely reflects the cost data for all fluids [17].

$$\dot{C}_1 + Z_{Total,Pump} = \dot{C}_2 \quad (15)$$

When a similar calculation is performed for the heat exchanger, Equation (16) is obtained. In this case, there are two inputs and two outputs, with one of the inputs being the geothermal cost. This cost value has been updated to the present day in line with the literature and is accepted as 1.6 $/GJ. The geothermal energy output cost is assumed to be c_6=c_5. Since the flow remains unchanged, the exergy cost also remains the same. The value of c_2 is known, and c_3 will be calculated.

$$\dot{C}_5 + \dot{C}_2 + \dot{Z}_{Total,HEX} = \dot{C}_3 + \dot{C}_6 \quad (16)$$

For the turbine, the calculation follows a similar approach, leading to Equation (17) [18]. In this scenario, there is one input and two outputs. One of the outputs here is the electricity cost. The c_3 stream is known, and as in the heat exchanger, $c_3 = c_4$ is assumed since the stream remains unchanged. The unit cost of the output power ($c_{electric}$) is calculated.

$$\dot{C}_3 + \dot{Z}_{Total,Turbine} = \dot{C}_4 + W_{net}.c_{electric} \quad (17)$$

The final component is the condenser, where the unit exergy cost calculation is performed. This component is essentially a type of heat exchanger [18]. The value of c_1 serves as the starting point and is constant. Since the entering cooling water is at ambient conditions, its exergy cost is considered zero. In reality, this water does have a cost, but since it has zero exergy, it is assumed to be zero. The exergy cost of the output, however, is assumed to be the same as the electrical exergy. In this way, the cost of the discharged exergy is represented in parallel with the work produced.

$$\dot{C}_4 + \dot{C}_7 + \dot{Z}_{Total,Condenser} = \dot{C}_1 + \dot{C}_8 \quad (18)$$

The initial investment costs of the components are determined in proportion to their sizes using Equations (19), (20), and (21) below. The condenser and evaporator are considered two heat exchangers with similar flow configurations. For these systems, the heat transfer coefficient of the heat exchanger is assumed to be 0.25 kW/m², and the required areas are calculated accordingly.

$$\dot{Z}_{CI,Pump} = 1120\left(w_p\right)^{0.8} \quad [19] \quad (19)$$

$$\dot{Z}_{CI,Turbine} = 4405\left(w_T\right)^{0.7} \quad [20] \quad (20)$$

$$\dot{Z}_{CI,HEX} = 2681\left(A_{HEX}\right)^{0.59} \quad [21] \quad (21)$$

3. Results and discussions

Both thermodynamic and thermo-economic analyses were conducted, and for each case, the thermodynamic properties and unit exergy costs of the working fluids were calculated. The phase table for R-134a, the first of these fluids, is provided in Table 1. The system operates with a working fluid flow rate of 108 kg/s and a turbine inlet pressure of 2800 kPa. The condenser pressure is 500 kPa, and the cooling water flow rate in the condenser is calculated as 525.6 kg/s.

Table 1. R-134a state-property table

	m (kg/s)	T (K)	P (kPa)	h (kj/kg)	s (kJ/kg.K)	c ($/GJ)
1	108	288.9	500	73.328	0.2802	6.00
2	108	290.2	2800	75.509	0.2814	6.30
3	108	373.3	2800	309.324	0.9652	4.21
4	108	307.5	500	277.132	0.9838	4.21
5	150	383.1	143.3	461.331	1.4190	1.60
6	150	343.1	143.3	292.984	0.9549	1.60
7	525.6	284.1	100	46.228	0.1656	0.00
8	525.6	294.1	100	88.106	0.3104	6.94

Another fluid planned for use in the system is isopentane. The phase properties of this fluid are provided in Table 2. The turbine inlet pressure has been updated in parallel with the evaporation point. This adjustment aims to select the highest possible pressure that can be achieved by evaporating the geothermal water at 383 K using a heat exchanger. A value of 710 kPa has been accepted as the high pressure. In the developed model, the pinch temperature for the heat exchanger has also been calculated, ensuring the temperature variation curves for the heat exchanger are accurately formed. Similarly, the condenser inlet pressure has been modified and adjusted to suit the fluid, with 90 kPa being accepted as the low pressure. The working fluid flow rate corresponding to all these values is taken as 54.8 kg/s. The temperature, enthalpy, entropy, and unit exergy costs appropriate for these conditions can be obtained from the table. The condenser cooling water flow rate is calculated as 520.6 kg/s.

Table 2. Isopentane state-property table

	m (kg/s)	T (K)	P (kPa)	h (kj/kg)	s (kJ/kg.K)	c ($/GJ)
1	54.8	297.6	90	-351.240	-1.6940	6.00
2	54.8	297.9	710	-350.054	-1.6930	12.77
3	54.8	373.1	710	110.749	-0.4007	2.22
4	54.8	327.5	90	46.596	-0.3658	2.22
5	150	383.1	143.3	461.331	1.4190	1.60
6	150	343.1	143.3	292.984	0.9549	1.60
7	520.6	284.1	100	46.228	0.1656	0.00
8	520.6	294.1	100	88.106	0.3104	0.57

A phase property table for n-Pentane has been created. Within this temperature range, n-Pentane operates at lower pressures than other fluids. The turbine inlet pressure is set at 550 kPa, and the condenser inlet pressure is taken as 80 kPa. At a pressure of 80 kPa, the saturation temperature is sufficiently far from the pinch point temperature. Although it is technically possible to further reduce the pressure for n-pentane, operation under high vacuum conditions has not been deemed practical. In practice, while there are power plants operating under vacuum conditions, extremely high vacuum pressures were not considered for this case. The working fluid mass flow rate is assumed to be 53 kg/s. Data set was calculated and showed in Table 3. The condenser water inlet flow rate is calculated as 526.6 kg/s according to these assumptions.

Table 3. n-Pentane state-property table

	m (kg/s)	T (K)	P (kPa)	h (kj/kg)	s (kJ/kg.K)	c ($/GJ)
1	53	302.2	80	7.427	0.0257	6.00
2	53	302.5	550	8.324	0.0261	12.04
3	53	373	550	484.776	1.3610	2.22
4	53	332	80	423.551	1.3930	2.22
5	150	383.1	143.3	461.331	1.4190	1.60
6	150	343.1	143.3	292.984	0.9549	1.60
7	526.6	284.1	100	46.228	0.1656	0.00
8	526.6	294.1	100	88.106	0.3104	4.73

When a state and thermodynamic property table is created for the refrigerant R-12, Table 4 is obtained. The turbine inlet pressure and condenser inlet pressure are set at 3200 kPa and 670 kPa, respectively. The working fluid mass flow rate is determined to be 166 kg/s, while the condenser cooling water flow rate is calculated as 528 kg/s.

Table 4. R-12 state-property table

	m (kg/s)	T (K)	P (kPa)	h (kj/kg)	s (kJ/kg.K)	c ($/GJ)
1	166	299.2	670	60.712	0.2272	6.00
2	166	301.5	3200	62.989	0.2347	6.68
3	166	373	3200	215.110	0.6599	4.20
4	166	299.2	670	193.911	0.6724	4.20
5	150	383.1	143.3	461.331	1.4190	1.60
6	150	343.1	143.3	292.984	0.9549	1.60
7	528	284.1	100	46.228	0.1656	0.00
8	528	294.1	100	88.106	0.3104	6.91

R-32 is another refrigerant tested in the system. The optimal pressure range for R-32 is between 1600 kPa and 5400 kPa, which is higher compared to most other fluids. The boiling point at the same pressure is considerably lower than that of other fluids. The working fluid mass flow rate is 84 kg/s, and the condenser cooling water flow rate is calculated as 537.7 kg/s. All these detailed results are provided in Table 5.

Table 5. R-32 state-property table

	m (kg/s)	T (K)	P (kPa)	h (kj/kg)	s (kJ/kg.K)	c ($/GJ)
1	84	296.1	1600	241.736	1.1440	6.00
2	84	299.1	5400	246.348	1.1460	6.68
3	84	372.8	5400	546.967	2.0270	4.20
4	84	296.1	1600	509.794	2.0490	4.20
5	150	383.1	143.3	461.331	1.4190	1.60
6	150	343.1	143.3	292.984	0.9549	1.60
7	537.7	284.1	100	46.228	0.1656	0.00
8	537.7	294.1	100	88.106	0.3104	8.11

Isobutane is the final working fluid proposed for use in the system. The state-property results of this fluid can be obtained from Table 6. The turbine inlet pressure is set at 1900 kPa, and the condenser inlet pressure is 300 kPa. The working fluid mass flow rate in the cycle is 58.5 kg/s, and the cooling water mass flow rate is calculated as 519.9 kg/s.

Table 6. Isobutane state-property table

	m (kg/s)	T (K)	P (kPa)	h (kj/kg)	s (kJ/kg.K)	c ($/GJ)
1	58.5	292.9	300	246.725	1.1640	6.00
2	58.5	293.9	1900	250.108	1.1660	6.40
3	58.5	372.9	1900	681.766	2.3950	3.42
4	58.5	313.7	300	618.906	2.4300	3.42
5	150	383.1	143.3	461.331	1.4190	1.60
6	150	343.1	143.3	292.984	0.9549	1.60
7	519.9	284.1	100	46.228	0.1656	0.00
8	519.9	294.1	100	88.106	0.3104	5.89

Based on the data from the tables arranged for all these different fluids, the net energy and unit energy costs have been calculated separately. Additionally, the system's energy and exergy efficiencies are also presented. All these systems can be compared in Table 7. The systems that generate the most energy is those using isopentane and isobutane. The lowest unit energy cost is achieved with isopentane. Systems using either isobutane or isopentane stand out in terms of both energy and exergy efficiency. These results are consistent with those found by Yılmaz [13,14]. A very close value of 2.75 MW was obtained for R-134a.

Table 7. Comparative results, net power output, unit cost of energy, energy and exergy efficiency

	Net Power (kW)	Unit Cost of Energy ($/kWh)	Energy Effciency (%)	Exergy Effciency (%)
R-134a	2755	0.02497	10.91	31.09
Isopentane	2933	0.01644	11.61	33.10
N-Pentane	2718	0.01702	10.76	30.67
R-12	2670	0.02487	10.57	30.13
Isobutane	2958	0.02120	11.71	33.37
R-32	2325	0.02922	9.21	26.24

Fluctuations in geothermal water temperature can occur from time to time. Through parametric analysis, the response of the fluids to changing geothermal water temperatures can be observed. The first data to be examined in the parametric analysis is the graph showing the variation of net energy produced with changing geothermal water temperature. The graph created for six different fluids is shown in Figure 3. The geothermal water temperature ranges from 373 K to 403 K. As the geothermal water temperature increases, the net energy output also increases. On the left side of the graph, between 373-383 K, isobutane and isopentane are at the top. In the 383-395 K range, isobutane is at the highest position. At higher temperatures, R-12 generates the most energy.

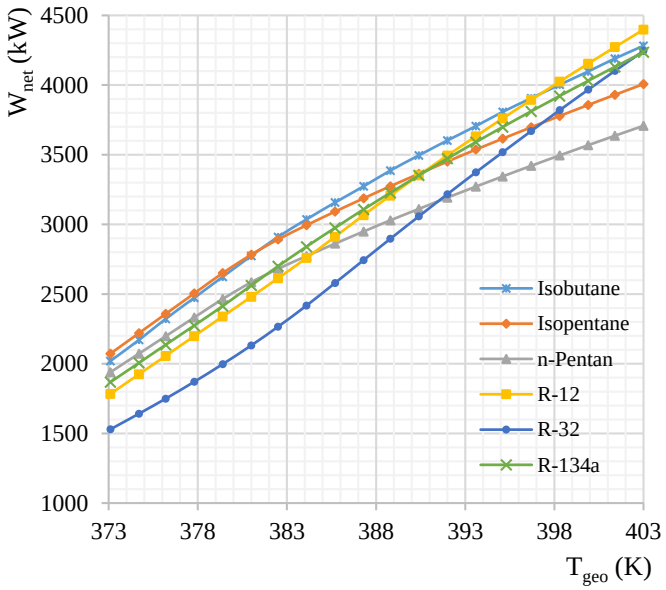

Figure 3. Net Energy Output of the Power Plant Versus Varying Geothermal Water Temperature

A similar graph has been created for the cost analysis. The variation of unit electricity cost with changing geothermal water temperature for different fluids can be observed in the graph in Figure 4. In this graph, the lowest cost is achieved with isopentane and n-pentane, while the highest cost is obtained with R-32.

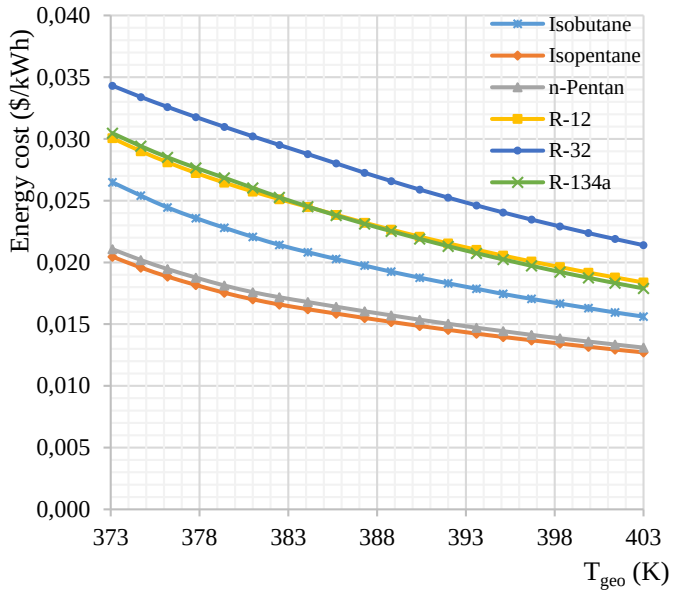

Figure 4. Unit Energy Cost Versus Varying Geothermal Water Temperature

4. Conclusions

The study investigates how different fluids react within the operational range for potential use in the Afyon geothermal power plant. R-134a is an actively used fluid. Additionally, fluids like isopentane, n-pentane, isobutane, R-12, and R-32, which can operate at similar

temperatures, were evaluated for the model.

Isobutane ranks among the top performers across all temperature values. Fluids with lower mass flow rates and smaller pressure differences appear more efficient, producing more energy. Moreover, as the mass flow decreases, costs are reduced. However, as the mass flow rate decreases, the system's sensitivity increases significantly, leading to larger responses to minor changes and fluctuations. This highlights the necessity for highly precise control units in real-world system designs.

R-134a, the fluid currently in use, provides an average response. Its performance data are not at the extremes for either mass flow or operating pressures compared to other fluids. However, geothermal water wells in the region with higher temperatures (~430 K) are occasionally encountered. If the system is modified for slightly higher temperatures, fluids like R-12 and R-32 could be considered. Furthermore, fluids like R-245fa could also be tested. This study is expected to guide future modification plans. However, detailed optimization for each fluid is essential if deemed necessary.

In this study, evaporation and condensation temperatures were kept as close to the limits as possible. However, greater energy production could be achieved by optimizing intermediate temperatures, which could be a significant step for better decision-making and system improvement in the future. clarity of all figures is extremely important.

Nomenclature

A_{HEX}	Heat exchanger Area
$\dot{c}_i$	Unit cost of exergy flow per mass
$\dot{C}$	Total cost of exergy flow
CRF	Cost recovery factor
$e\dot{x}$	Exergy flow per mass flow rate
$E\dot{x}$	Exergy of a flow
η_p	Pump isentropic efficiency
η_T	Turbine isentropic efficiency
h_i	Enthalpy of i-th state
i	Interest rate
$\dot{m}_i$	Mass flow rate of i-th state
n	Number of period
ORC	Organic rankine cycle
P_i	Pressure of the i-th state
φ	Maintenance factor
v_i	Specific volume
$\dot{w}_P$	Pump work
$\dot{w}_T$	Turbine work

Subscript

geo	Geothermal
k	Component
s	Entropi
iso	Isontropic
wf	Working fluid

Conflict of Interest Statement

Author declares that there is no conflict of interest in the study.

References

1. Lund, J. W., Huttrer, G. W., & Toth, A. N. (2022). Characteristics and trends in geothermal development and use, 1995 to 2020. Geothermics, 105, 102522. https://doi.org/10.1016/j.geothermics.2022.102522
2. Wang, E. H., Zhang, H. G., Fan, B. Y., Ouyang, M. G., Zhao, Y., & Mu, Q. H. (2011). Study of working fluid selection of organic Rankine cycle (ORC) for engine waste heat recovery. Energy, 36(5), 3406-3418. https://doi.org/10.1016/j.energy.2011.03.041
3. Liu, Y., Sun, W., & Liu, X. (2024). Greening the organic Rankine cycles: low-global warming potential working fluids for low-temperature waste heat recovery. International Journal of Exergy, 45(1-2), 126-143. https://doi.org/10.1504/IJEX.2024.141686
4. Li, B., Xie, H., Sun, L., Gao, T., Xia, E., Liu, B., ... & Long, X. (2024). Advanced exergy analysis and multi-objective optimization of dual-loop ORC driven by LNG cold energy and geothermal energy. Renewable Energy, 122164. https://doi.org/10.1016/j.renene.2024.122164
5. Daniarta, S., Imre, A. R., & Kolasiński, P. (2024). A novel approach to district heating: using a two-phase expander in reversible heat pump-Organic Rankine Cycle system. In Proceedings of the 7th International Seminar on ORC Power System:(ORC2023) (pp. 169-175). Editorial Universidad de Sevilla. https://dx.doi.org/10.12795/9788447227457
6. Xia, X., Zhang, H., Wang, Z., Yang, C., Sun, T., & Peng, B. (2024). Performance comparison of two ORC-VCR system configurations using pure/mixture working fluids based on multi-objective optimization. Applied Thermal Engineering, 255, 124027. https://doi.org/10.1016/j.applthermaleng.2024.124027
7. Feng, J., Yan, Y., Zhao, L., & Dong, H. (2024). Energy, Exergy, and Economic Performance Comparison and Parametric Optimization of Organic Rankine Cycles Using Isobutane, Isopentane, and Their Mixtures for Waste Heat Recovery. Energies (19961073), 17(23). https://doi.org/10.3390/en17235893
8. Liang, Z., Zheng, G., Wu, G., Pan, Z., Hu, Z., Xu, M., & Chen, H. (2024). Thermodynamic performance of organic Rankine cycle based pumped thermal energy storage system with different working fluids. Heliyon. https://doi.org/10.1016/j.heliyon.2024.e41052
9. Rachmat, A., Pansawati, I. S., Agustin, Y., Surachman, A., Sutardi, T., & Suyanto, S. (2024, November). Multi-Objective optimization of a combined double flash–Binary cycle for Wayang Windu geothermal power plant based on exergy and economics. In AIP Conference Proceedings (Vol. 3215, No. 1). AIP Publishing. https://doi.org/10.1063/5.0235648
10. Hou, Z., Imechoui, I., Chong, P. L., Guo, P., Deng, Y., & Gao, Y. (2024). Enhancing exergy and economical performance of a waste heat power generation system: Multi-objective optimization and comparative analysis. Journal of Cleaner Production, 482, 144235. https://doi.org/10.1016/j.jclepro.2024.144235
11. Özcan, Z., & Ekici, Ö. (2021). A novel working fluid selection and waste heat recovery by an exergoeconomic approach for a geothermally sourced ORC system. Geothermics, 95, 102151. https://doi.org/10.1016/j.geothermics.2021.102151
12. Şahin, C. (2016). Düşük sıcaklıklı jeotermal sahalarda organik rankin çevrimi (ORC) ile elektrik enerjisi üretiminde Afyon Jeotermal Elektrik Üretim AŞ modellemesi (Master's thesis, Fen Bilimleri Enstitüsü).

13. Yılmaz, C. (2020). Performance Evaluation of Afyon Geothermal Power Plant with Low Grade Energy Sources. Konya Journal of Engineering Sciences, 8(3), 448-465. https://doi.org/10.36306/konjes.627174
14. Yılmaz, C. (2020). Improving performance and thermoeconomic optimization of an existing binary geothermal power plant: A case study. Isı Bilimi ve Tekniği Dergisi, 40(1), 37-51.
15. Sen, O., Guler, O. F., Yilmaz, C., & Kanoglu, M. (2021). TherModynamic Modeling and Analysis of a Solar and Geothermal Assisted Multi-Generation Energy System. Energy Conversion and Management, 239, 114186. https://doi.org/10.1016/j.enconman.2021.114186
16. Cengel, Y. A., Boles, M. A., & Kanoğlu, M. (2011). *Thermodynamics: an engineering approach* (Vol. 5, p. 445). New York: McGraw-hill.
17. Bejan, A., Tsatsaronis, G., & Moran, M. J. (1995). Thermal design and optimization. John Wiley & Sons.
18. Guler, O. F., Sen, O., Yilmaz, C., & Kanoglu, M. (2022). Performance evaluation of a geothermal and solar-based multigeneration system and comparison with alternative case studies: Energy, exergy, and exergoeconomic aspects. Renewable Energy, 200, 1517-1532. https://doi.org/10.1016/j.renene.2022.10.064
19. Özahi, E., & Tozlu, A. (2020). Optimization of an adapted Kalina cycle to an actual municipal solid waste power plant by using NSGA-II method. Renewable Energy, 149, 1146-1156. https://doi.org/10.1016/j.renene.2019.10.102
20. Mahmoudi, S. M. S., Pourreza, A., Akbari, A. D., & Yari, M. (2016). Exergoeconomic evaluation and optimization of a novel combined augmented Kalina cycle/gas turbine-modular helium reactor. Applied Thermal Engineering, 109, 109-120. https://doi.org/10.1016/j.applthermaleng.2016.08.011
21. Mosaffa, A. H., Mokarram, N. H., & Farshi, L. G. (2017). Thermoeconomic analysis of a new combination of ammonia/water power generation cycle with GT-MHR cycle and LNG cryogenic exergy. Applied Thermal Engineering, 124, 1343-1353. https://doi.org/10.1016/j.applthermaleng.2017.06.126